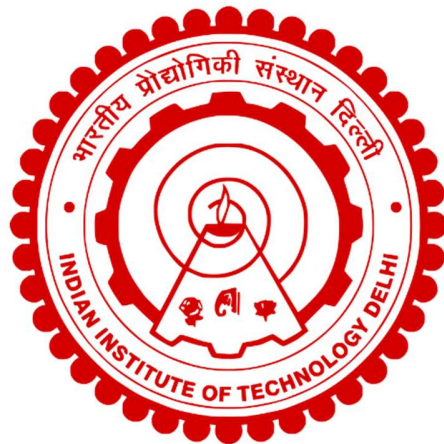


**MODELLING AND ANALYSIS OF HIGHER ORDER MODES IN  
OPTICAL FIBERS & COMPONENTS**

**AJAY KUMAR**



**DEPARTMENT OF PHYSICS  
INDIAN INSTITUTE OF TECHNOLOGY DELHI  
JULY 2025**

© Indian Institute of Technology Delhi (IITD), New Delhi, 2025

**MODELLING AND ANALYSIS OF HIGHER ORDER MODES IN  
OPTICAL FIBERS & COMPONENTS**

*by*

**AJAY KUMAR**

**Department of Physics**

*Submitted*

*in fulfilment of the requirements of the degree of*

*Doctor of Philosophy*

*to the*



**DEPARTMENT OF PHYSICS  
INDIAN INSTITUTE OF TECHNOLOGY DELHI  
JULY 2025**

*To my Family*

## CERTIFICATE

---

---

This is to certify that the Thesis entitled “**MODELLING AND ANALYSIS OF HIGHER ORDER MODES IN OPTICAL FIBERS & COMPONENTS**” being submitted by **Mr. Ajay Kumar** to the Department of Physics, Indian Institute of Technology Delhi, for the award of the degree of ‘**Doctor of Philosophy**’ is a record of Bonafide work carried out by him. He has worked under our supervision and guidance and has fulfilled the requirements for the submission of the thesis, which in our opinion has reached the requisite standard.

The results contained in this work have not been submitted, in part or fully, to any other University or Institute for the award of any degree or diploma to the best of our knowledge.



**Prof. Anurag Sharma**

Department of Physics,

Indian Institute of Technology Delhi.

Hauz Khas, New Delhi-110016

India



**Prof. R. K. Varshney**

Department of Physics,

Indian Institute of Technology Delhi.

Hauz Khas, New Delhi-110016

India



## ACKNOWLEDGEMENTS

---

---

This thesis has been completed with the blessings of my beloved parents. The successful completion of this doctoral work was made possible by the support of many individuals, to whom I extend my heartfelt gratitude.

First, I express my deepest gratitude to my supervisor, **Prof. Anurag Sharma**, for his invaluable guidance, unwavering support, and constant encouragement throughout my research journey. His insightful suggestions, mentorship, and emphasis on independent thinking have greatly enhanced my confidence, presentation skills, and understanding of the subject. His patience and willingness to help during challenges were truly inspiring. Discussions with him have been stimulating and rewarding, shaping me both personally and professionally. I am deeply thankful for his role in making my Ph.D. journey pleasant and memorable.

I extend my heartfelt gratitude to my co-supervisor, **Prof. R K Varshney**, for his unwavering support and understanding. His interactions have consistently inspired me to push beyond my limits. I am deeply grateful to Prof. M R Shenoy for his valuable advice, guidance, support and encouragement to complete my research work. Special thanks to Prof. Joby Joseph for his illuminating discussions and support. My sincere thanks to Prof. Arun Kumar for his encouraging discussions and clarifications that went far beyond the scope of coursework.

I would also like to acknowledge the unrelenting support, guidance and inspiration provided by Prof. Ajoy Ghatak, Prof. K Thyagarajan and the faculty members of the fiber optics group at IIT Delhi. I am thankful to IIT Delhi for all the infrastructure support and the financial assistance given to me for attending and presenting my work at reputed national and international conferences. My scholarship was funded by the Council of Scientific and Industrial

Research (CSIR), Ministry of Science and Technology, Government of India, for which I am extremely grateful.

I would like to express my sincere thanks to Dr. Ramesh Kumar for his valuable advice and unwavering support throughout my computational work, and to Dr. Sugeet Sunder for the many enjoyable discussions, both academic and beyond. My gratitude also extends to my lab mate Pratiksha, with whom I have shared the common computational system. Additionally, I am grateful to the members of the OSA and SPIE student chapters for their support and collaboration.

I express my heartfelt gratitude to Prof. Fakir Chand, Prof. Rajesh Kharab and Prof. R. K. Moudgil and all the esteemed faculty members of the Department of Physics, Kurukshetra University, Kurukshetra for their constant encouragement, and profound insights.

I am deeply grateful to all my teachers, whose guidance has been instrumental in bringing me to this point. This thesis would not have been possible without the unwavering support and encouragement of my parents, Smt. Bhateri Devi and Sh. Basau Ram. This thesis is a result of their sacrifices and blessings.

**Date: 07/07/2025**

*Ajay Kumar*

**Ajay Kumar**

## ABSTRACT

---

---

Over the past two to three decades, optoelectronic devices have become increasingly important. Developing these devices requires effective modeling and analysis techniques, as analytical solutions are not feasible for non-uniform structures, making numerical methods essential. Optical fibers are a very important class of components used in optoelectronics and optical communication. Optical fibers are classified by modes: single-mode fibers (SMFs) carry only the fundamental mode, while multimode fibers (MMFs) support higher-order modes (HOMs) also. HOMs enhance communication capacity through mode-division multiplexing and enable advanced sensing.

In this thesis, for optical fiber and components, cylindrical coordinates are used to describe Maxwell's equations and wave equations. Propagation methods solve the wave equation, with various approaches developed for beam propagation in photonic structures. Scalar wave approximation offers efficient results in low index contrast structures, and solutions vary based on the specific parameters of problem. We have developed an efficient method for wave propagation in azimuthally symmetric fiber structures, supporting both paraxial and non-paraxial wave propagation. The method reduces the scalar wave equation to 2D from 3D which requires only fewer sample (collocation) points, offering significant computational efficiency and accuracy. This method is applicable to all higher order modes including OAM modes.

We have examined the propagation of higher order modes in fiber tapers and fiber Bragg gratings (FM-FBGs) for sensing applications. It uses the split-step non-paraxial method to compute reflections and spectral responses. Our study on a fiber sensor based on FM-FBG for simultaneous temperature and refractive index measurement using  $LP_{01}$  and  $LP_{11}$  modes shows a

good agreement with experiments.  $LP_{11}$  mode has higher refractive index sensitivity, while temperature sensitivity is similar for both. We have also examined the issue of cross-sensitivity between the two parameters in simultaneous measurement. We have concluded that cross-sensitivity is very small and largely unreliable to quantify. Sensor tip modification improves temperature sensitivity by 15.76% for  $LP_{01}$  and 18.59% for  $LP_{11}$ . The effects of ring-core fiber parameters on mode coupling, effective area, and differential mode delay have also been analyzed. Finally, we have proposed a stable optical tweezer probe using a ring-core fiber and graded-index multimode fiber, which supports stable OAM modes.

We have proposed a new method for obtaining mode and the modal loss in leaky guiding structure. The leaky mode is obtained as the limiting-guided mode of the given leaky structure. The loss is obtained by propagating this mode through the leaky structure. The mode computation and the propagation loss have been carried out using the collocation method. We have optimized a Bragg fiber with nine periodic bilayers of low and high refractive index to improved mode confinement. The structure keeps the mode well-confined for wavelengths from  $0.6 \mu m$  to  $1.242 \mu m$ , with very low loss. Higher-order modes leak out and have been handled with the ABC boundary conditions.

Finally, for the modelling of the structures with unevenly distributed guiding regions, redistributing collocation points is necessary. This has been achieved with a transformation function that ensures a one-to-one correspondence between the transformed and real space. We have demonstrated improved accuracy in modal computation for large core Bragg fiber. We have also shown that the solid core Bragg fibers can also efficiently modelled using this variable transformed collocation method.

## सार

---

पिछले दो से तीन दशकों में, ऑप्टोइलेक्ट्रॉनिक डिवाइस बहुत महत्वपूर्ण हो गए हैं। इन डिवाइस को विकसित करने के लिए प्रभावी मॉडलिंग और विश्लेषण तकनीकों की आवश्यकता होती है, क्योंकि गैर-समान संरचनाओं के लिए विश्लेषणात्मक समाधान संभव नहीं हैं, जिससे संख्यात्मक विधियाँ आवश्यक हो जाती हैं। ऑप्टिकल फाइबर ऑप्टोइलेक्ट्रॉनिक्स और ऑप्टिकल संचार में उपयोग किए जाने वाले घटकों का एक बहुत ही महत्वपूर्ण वर्ग है। ऑप्टिकल फाइबर को मोड के आधार पर वर्गीकृत किया जाता है: सिंगल-मोड फाइबर (SMF) केवल मूल मोड को ले जाते हैं, जबकि मल्टीमोड फाइबर (MMF) उच्च-क्रम मोड (HOM) का भी समर्थन करते हैं। HOM मोड-डिवीजन मल्टीप्लेक्सिंग के माध्यम से संचार क्षमता को बढ़ाते हैं और उन्नत संवेदन को सक्षम करते हैं।

इस थीसिस में, ऑप्टिकल फाइबर और घटकों के लिए, मैक्सवेल के समीकरणों और तरंग समीकरणों का वर्णन करने के लिए बेलनाकार निर्देशांक का उपयोग किया जाता है। प्रसार विधियाँ तरंग समीकरण को हल करती हैं, जिसमें फोटोनिक संरचनाओं में बीम प्रसार के लिए विभिन्न दृष्टिकोण विकसित किए गए हैं। स्केलर तरंग सन्निकटन कम सूचकांक विपरीत संरचनाओं में कुशल परिणाम प्रदान करता है, और समाधान समस्या के विशिष्ट मापदंडों के आधार पर भिन्न होते हैं। हमने एजिमुथली सममित फाइबर संरचनाओं में तरंग प्रसार के लिए एक कुशल विधि विकसित की है, जो पैराक्सियल और गैर-पैराक्सियल तरंग प्रसार दोनों का समर्थन करती है। यह विधि स्केलर तरंग समीकरण को 3D से 2D तक कम कर देती है जिसके लिए केवल कम नमूना (कोलोकेशन) बिंदुओं की आवश्यकता होती है, जो महत्वपूर्ण कम्प्यूटेशनल दक्षता और सटीकता प्रदान करता है। यह विधि OAM मोड सहित सभी उच्च क्रम मोड पर लागू होती है।

हमने संवेदन अनुप्रयोगों के लिए फाइबर टेपर और फाइबर ब्रैग ग्रेटिंग (FM-FBGs) में उच्च क्रम मोड के प्रसार की जांच की है। यह प्रतिबिंबों और वर्णक्रमीय प्रतिक्रियाओं की गणना करने के लिए विभाजित-चरण गैर-पैराक्सियल विधि का उपयोग करता है।  $LP_{01}$  और  $LP_{11}$  मोड का उपयोग करके एक साथ तापमान और अपवर्तक सूचकांक माप के लिए FM-FBG पर आधारित फाइबर संसर पर हमारा अध्ययन प्रयोगों के साथ एक अच्छा समझौता दिखाता है।  $LP_{11}$  मोड में उच्च अपवर्तक सूचकांक संवेदनशीलता है, जबकि तापमान संवेदनशीलता दोनों के लिए समान है। हमने एक साथ माप में दो मापदंडों के बीच क्रॉस-सेंसिटिविटी के मुद्दे की भी जांच की है। हमने निष्कर्ष निकाला है कि क्रॉस-सेंसिटिविटी बहुत छोटी है और इसे मापना काफी हद तक अविश्वसनीय है। अंत में, हमने रिंग-कोर फाइबर और ग्रेडेड-इंडेक्स मल्टीमोड फाइबर का उपयोग करके एक स्थिर ऑप्टिकल ट्विजर जांच का प्रस्ताव दिया है, जो स्थिर OAM मोड का समर्थन करता है।

हमने लीकी गाइडिंग संरचना में मोड और मोडल हानि प्राप्त करने के लिए एक नई विधि प्रस्तावित की है। लीकी मोड को दी गई लीकी संरचना के सीमित-निर्देशित मोड के रूप में प्राप्त किया जाता है। लीकी संरचना के माध्यम से इस मोड को प्रसारित करके हानि प्राप्त की जाती है। मोड गणना और प्रसार हानि को कॉलोकेशन विधि का उपयोग करके किया गया है। हमने कम और उच्च अपवर्तक सूचकांक के नौ आवधिक द्विपरतों के साथ एक ब्रैग फाइबर को बेहतर मोड कारावास के लिए अनुकूलित किया है। संरचना 0.6 माइक्रोन से 1.242 माइक्रोन तक तरंग दैर्ध्य के लिए मोड को अच्छी तरह से सीमित रखती है, बहुत कम हानि के साथ। उच्च-क्रम मोड लीक हो जाते हैं और उन्हें एबीसी सीमा स्थितियों के साथ संभाला गया है।

अंत में, असमान रूप से वितरित मार्गदर्शक क्षेत्रों वाली संरचनाओं के मॉडलिंग के लिए, कॉलोकेशन बिंदुओं को फिर से वितरित करना आवश्यक है। यह एक परिवर्तन फंक्शन के साथ प्राप्त किया गया है जो परिवर्तित और वास्तविक स्थान के बीच एक-से-एक पत्राचार सुनिश्चित करता है। हमने बड़े कोर ब्रैग फाइबर

के लिए मोडल गणना में बेहतर सटीकता का प्रदर्शन किया है। हमने यह भी दर्शाया है कि ठोस कोर ब्रैग फाइबर को भी इस परिवर्तनीय रूपांतरित कोलोकेशन विधि का उपयोग करके कुशलतापूर्वक मॉडल किया जा सकता है।



# CONTENTS

---

---

<b>CERTIFICATE</b>	<b>i</b>
<b>ACKNOWLEDGEMENTS</b>	<b>iii-iv</b>
<b>ABSTRACT</b>	<b>v-ix</b>
<b>CONTENTS</b>	<b>xi-xv</b>
<b>SYMBOLS &amp; THEIR DESCRIPTION</b>	<b>xvii</b>
<b>ABBREVIATIONS</b>	<b>xix</b>
<b>LIST OF FIGURES</b>	<b>xx-xxv</b>
<b>LIST OF TABLES</b>	<b>xxvi</b>
<b>CHAPTER I: Introduction</b>	<b>1-13</b>
1.1 The Study of Light	1
1.1.1 Photonics over Electronics	2
1.2 Optical Fibers and Waveguides	2
1.2.1 Higher Order Modes & OAM Modes	3
1.3 Theoretical and Computational Modeling	4
1.3.1 Collocation Framework	6
1.3.2 Computational Tool: MATLAB	7
1.4 Approach Followed in the Thesis Work	7
1.5 Contributions in the Thesis	8
1.6 Organization of Proposed Thesis	9
<b>CHAPTER II: Mathematical Preliminaries</b>	<b>15-29</b>
2.1 Introduction	15

2.2	The Wave Equations	16
2.2.1	Maxwell's Equations and the Wave Equation	17
2.2.2	Weak Guidance Approximation and the Scalar Wave Equation	18
2.2.3	Scalar Wave Equation for Cylindrical Geometries	21
2.2.4	Scalar Wave Equation for Optical Fibers	21
2.3	Solution Methods for Scalar Wave Equation	24
2.4	Orthogonal Collocation Method	25
2.4.1	Orthogonal Polynomials	26
2.4.2	Collocation Method	26
2.5	Conclusion	29
<b>CHAPTER III: Modal and Propagation Methods for <math>LP_{lm}</math> Modes</b>		<b>31-48</b>
3.1	Introduction	31
3.2	Radial Collocation Method for $LP_{lm}$ Modes	33
3.2.1	Choice of Scaling Factor ' $\alpha$ '	36
3.2.2	Mode Computations	36
3.3	Propagation Methods	37
3.3.1	Paraxial Propagation Method	38
3.3.2	Non-Paraxial Propagation Method	40
3.3.3	Step-Size ( $\Delta z$ ) in Propagation Methods	41
3.3.4	Propagation of Arbitrary Fields	42
3.4	Analysis of Propagated Field	43
3.4.1	Higher Order $LP_{lm}$ Modes	44
3.4.2	Orbital Angular Momentum ( $OAM_{\pm l1}$ ) Modes	44

3.4.3	Fractional Power in Core and Calculation of Loss	45
3.4.4	Reflection/Transmission Coefficients	45
3.5	Efficiency of the Method	46
3.6	Conclusions	48
<b>CHAPTER IV: Applications of the Radial Collocation Method</b>		<b>50-63</b>
4.1	Introduction	50
4.2	Few-Mode Step Index Fibers	51
4.3	$LP_{lm}$ Modes in Ring Core Fibers	53
4.3.1	Modal Properties of OAM Modes in RCF	54
4.3.2	Tapered Ring Core Fibers	55
4.4	Design of RCF-GIMF Based Optical Tweezers Probe	58
4.5	Few-Mode Fiber Bragg Grating	60
4.6.	Conclusions	62
<b>CHAPTER V: Modelling of Few-Mode Fiber Bragg Grating Sensors</b>		<b>65-84</b>
5.1	Introduction	65
5.2	Basic Design of FBG Sensors	66
5.2.1	Modelling of FM-FBG Sensors	67
5.3	Sensing	70
5.3.1	Refractive Index Sensing	70
5.3.2	Temperature Sensing	72
5.3.3	Simultaneous Measurement	73
5.4	Cross-Sensitivity Analysis	75
5.5	Improvement of Sensitivity	80

5.5.1	Composite Core	80
5.5.2	Length Optimization	83
5.6	Conclusions	84
<b>CHAPTER VI: Leaky Structures and Leakage Loss</b>		<b>86-100</b>
6.1	Introduction	86
6.2	Guided and Leaky Modes	87
6.3	Modelling of Leaky Fiber Structures	89
6.3.1	Computing Limiting-guided Mode	89
6.3.2	Propagation and Computation of Loss	91
6.4	Applications	92
6.4.1	Single Mode Depressed Inner Cladding Fibers	92
6.4.2	Few-Mode Depressed Inner Cladding Fibers	96
6.4.3	Trench-assisted Large Mode Area Single Mode Fibers	98
6.5	Conclusions	100
<b>CHAPTER VII: Modelling and Analysis of Bragg Fibers</b>		<b>102-120</b>
7.1	Introduction	102
7.2	Modelling and Propagation Analysis of Bragg Fibers	103
7.2.1	Analysis of Solid Core Bragg Fibers	103
7.2.2	Modal Field	104
7.2.3	Optimizing the Layers Thickness	106
7.2.4	Gaussian Beam Propagation	108
7.3	Hollow Core Bragg Fibers	110
7.3.1	Variable Transform Collocation Method	111

7.3.2	Propagation Characteristics of Hollow Core Fibers	115
7.3.3	Modelling of Solid Core Bragg Fiber with VTCM	117
7.4	Conclusions	119
<b>CHAPTER VIII: Conclusion and Scope for Future Work</b>		<b>122-124</b>
8.1	Conclusions	122
8.2	Scope for Future Work and Proposed Extensions	123
<b>APPENDIX</b>		<b>126-141</b>
<b>REFERENCES</b>		<b>142-150</b>
<b>LIST OF PUBLICATIONS</b>		<b>151-153</b>
<b>AUTHOR'S BIOGRAPHY</b>		<b>154</b>



## SYMBOLS AND THEIR DESCRIPTIONS

---

Symbol	Description	Symbol	Description
$E$	Electric field	$\phi_n^l(r)$	Collocation function
$D$	Electric displacement	$c_n(z)$	Expansion coefficients
$H$	Magnetic field	$\psi(r)$	Radial field variation
$B$	Magnetic intensity	$\Phi(\varphi)$	Azimuthal field variation
$E_z$	z-component of electric field	$\varphi$	Azimuthal angle
$E_y$	y-component of electric field	$L_n^l(r)$	Associated-Laguerre functions
$E_x$	x-component of electric field	$\alpha$	Scaling factor
$H_z$	z-component of magnetic field	$\chi$	Wave propagating without fast-varying phase part
$H_y$	y-component of magnetic field	$w$	Weight factor
$H_x$	x-component of magnetic field	$\Delta z$	Step-size in propagation
$\epsilon$	Permittivity in dielectric medium	$\Gamma$	Attenuation constant
$\epsilon_0$	Permittivity in free space	$\delta n$	Refractive index modulation
$\mu$	Permeability of dielectric material	$\Lambda$	Grating period in FBG
$\mu_0$	Permeability in free space	$\xi$	Thermo-optic coefficient
$c$	Speed of light	$\alpha_T$	Thermal expansion coefficient
$\epsilon_r$	Relative permittivity	$k_n$	Refractive index sensitivity
$\mu_r$	Relative permeability	$k_T$	Temperature sensitivity
$v$	Velocity of light in medium	$Y$	Young's modulus of elasticity
$\lambda$	Wavelength	$\delta_{mn}$	Kronecker delta
$n_r$	Reference refractive index	$n_{eff}$	Effective refractive index
$n_c$	Refractive index of core	$P_{frac}$	Fractional power in core
$n_{cl}$	Refractive index of cladding	$d$	Thickness of ABC layer
$l$	Orbital angular momentum number	$g$	Gradient constant for GIMF
$\nabla$	Nabla or del operators	$\sigma$	Transformed variable
$\hbar$	Reduced Planck constant	$h(\sigma)$	Transformation
$k_0$	Free-space wave vector	$h'(\sigma)$	First derivative of transformation
$\omega$	Angular frequency	$h''(\sigma)$	2 <sup>nd</sup> derivative of transformation
$\beta$	Propagation constant	$U(\sigma)$	Transformed transverse field
$r_c$	Radius of core		



## ABBREVIATIONS

---

<b>Abbreviation</b>	<b>Full Form</b>
<b>ABC</b>	Absorbing Boundary Conditions
<b>BPM</b>	Beam Propagation Method
<b>DMD</b>	Differential Mode Delay
<b>FBGs</b>	Fiber Bragg Grating
<b>FD</b>	Finite Difference
<b>FE</b>	Finite Element
<b>FM-FBG</b>	Few-mode Fiber Bragg Grating
<b>FM-SIF</b>	Few-mode Step-Index Fibers
<b>FWHM</b>	Full Width at Half Maximum
<b>GIMF</b>	Graded-Index Multimode Fibers
<b>HOMs</b>	Higher-Order Modes
<b>LEDs</b>	Light-Emitting Diodes
<b>LMA</b>	Large Mode Area
<b>LPGs</b>	Long-Period Grating
<b>MDM</b>	Mode Division Multiplexing
<b>MMFs</b>	Multimode Fibers
<b>MM-SIF</b>	Multimode Step-Index Fibers
<b>OAM</b>	Orbital Angular Momentum
<b>PMP</b>	Polymethyl Pentane
<b>RCFs</b>	Ring Core Fibers
<b>RIU</b>	Refractive Index Unit
<b>SMFs</b>	Single-Mode Fibers
<b>SMS</b>	Single-mode-Multimode-single-mode
<b>SSNP</b>	Split-Step Non-Paraxial
<b>TMM</b>	Transfer Matrix Method
<b>VTCM</b>	Variable Transformed Collocation Method

## LIST OF FIGURES

Figure No.	Descriptive Caption of Figure	Page No.
Fig. 1.1	<i>Schematic of arbitrary waveguide</i>	3
Fig. 2.1	<i>Propagation of EM-wave with variation of E and B fields</i>	19
Fig. 2.2	<i>Representation of optical fiber in cylindrical coordinates</i>	21
Fig. 2.3	<i>Input modal field (Gaussian Beam) as linear combination of scaled associate-Laguerre-Gauss functions</i>	27
Fig. 3.1	<i>Schematic of wave propagation methods as marching algorithms</i>	38
Fig. 3.2	<i>Description of slowly varying envelope approximation</i>	39
Fig. 3.3	<i>Modal field profile for different LP<sub>lm</sub> modes in few-mode step index fiber</i>	44
Fig. 3.4	<i>OAM<sub>±1</sub> modes as linear combination of LP<sub>11</sub> modes and phase variation</i>	45
Fig. 3.5	<i>Efficiency of radial collocation method in terms of grid point in cartesian grid and radial grid for azimuthally symmetric structures</i>	47
Fig. 4.1	<i>Modes in step index fiber (a) the refractive index profile with different LP<sub>lm</sub> modes and (b) The intensity profile of different LP<sub>lm</sub> modes</i>	52
Fig. 4.2	<i>(a) Mode effective index <math>n_{eff}</math> as a function of V-number for FM-SIF-28. (b) Mode group index <math>n_{group}</math> as a function of V-number for few LP<sub>lm</sub> modes. The effective index for all modes lies between <math>n_c</math> and <math>n_{cl}</math>.</i>	52
Fig. 4.3	<i>Modes in RCF: the refractive index profile and the radial variation of the intensity of LP<sub>11</sub> or OAM<sub>+1</sub> (<math>n_{eff} = 1.44722</math>) mode and LP<sub>21</sub> or OAM<sub>+2</sub> (<math>n_{eff} = 1.44587</math>) mode. Insets show the schematic of the fiber</i>	53

and the cross-sectional intensity and phase profile of  $OAM_{+1}$  and  $OAM_{+2}$  modes.

- Fig. 4.4**  $OAM_{\pm lm}$  modes from  $LP_{lm}$  modes and phase profiles 54
- Fig. 4.5** Schematic of linear taper ring core fiber 55
- Fig. 4.6** Refractive index profile and the radial variation of various  $LP_{lm}$  modes for a ring core fiber **(a)** at the larger end and **(b)** at the smaller end. 56
- Fig. 4.7** Power fraction in the guiding region (core + ring) for various modes as a function of the propagation distance in a tapered RCF 57
- Fig. 4.8** Schematic of RCF-GIMF optical tweezer probe 59
- Fig. 4.9** Evolution of modal field intensity with propagation for  $OAM_{+1}$  and  $OAM_{+3}$  mode 59
- Fig. 4.10** Periodic variation of **(a)** power and **(b)** effective radius of  $OAM_{+1}$  and  $OAM_{+3}$  modes 60
- Fig. 4.11** Refractive index profile and the radial variation of various  $LP_{lm}$  modes in a FM-EBG. The inset shows a schematic of the FM-FBG and the index modulation over two periods. 61
- Fig. 4.12** The reflection spectra of the FM-FBG showing corresponding to different  $LP_{lm}$  mode. A small peak due to cross-coupling of  $LP_{01} - LP_{02}$  modes is also observed. 62
- Fig. 5.1** Modal intensity profile of  $LP_{01}$  and  $LP_{11}$  modes of FM-FBG. The inset shows a schematic FM-FBG with index modulation over two periods 67
- Fig. 5.2** Bragg wavelengths for  $LP_{01}$  and  $LP_{11}$  modes from phase-matching condition ( $\beta = \pi/\Lambda$ ) and from reflection spectra of FM-FBG. 68

<b>Fig. 5.3</b>	<i>Simulated results for fractional power in cladding (evanescent field) for air and water for LP<sub>01</sub> and LP<sub>11</sub> modes.</i>	69
<b>Fig. 5.4</b>	<i>Refractive index sensitivity (nm/RIU) with etching the core radius.</i>	69
<b>Fig. 5.5</b>	<i>Variation of difference in Bragg wavelength of LP<sub>01</sub> and LP<sub>11</sub> modes with a core radius for air and water as surrounding refractive index.</i>	70
<b>Fig. 5.6</b>	<b>(a)</b> <i>Reflection spectra of LP<sub>01</sub> and LP<sub>11</sub> modes with external refractive index</i> <b>(b)</b> <i>Shift in Bragg wavelengths for the LP<sub>01</sub> and the LP<sub>11</sub> with external refractive index. The temperature is kept at 22°C.</i>	71
<b>Fig. 5.7</b>	<b>(a)</b> <i>Reflection spectrum of LP<sub>01</sub> and LP<sub>11</sub> modes</i> <b>(b)</b> <i>Shift in Bragg wavelengths for the LP<sub>01</sub> and the LP<sub>11</sub> modes at different temperatures. The refractive index of the external medium is 1.3159.</i>	72
<b>Fig. 5.8</b>	<i>Simultaneous measurement of refractive index and temperature</i> <b>(a)</b> <i>Reflection spectra for LP<sub>01</sub> mode</i> <b>(b)</b> <i>Shift in <math>\lambda_B</math>(LP<sub>01</sub>)</i> <b>(c)</b> <i>Reflection spectra for LP<sub>11</sub> mode</i> <b>(d)</b> <i>Shift in <math>\lambda_B</math>(LP<sub>11</sub>)</i>	74
<b>Fig. 5.9</b>	<b>(a)</b> <i>Shift in Bragg wavelengths (broken curve) for the LP<sub>01</sub> with temperature for water as external medium (refractive index = 1.3159 and its slope (continuous curve)</i> <b>(b)</b> <i>The slope on an expanded scale.</i>	78
<b>Fig. 5.10</b>	<i>Cross-sensitivity in simultaneous measurement of refractive index and temperature</i>	78
<b>Fig. 5.11</b>	<i>Schematic of modified FM-FBGs with PMP layer and length optimization</i>	81
<b>Fig. 5.12</b>	<i>Temperature sensitivities of different modes in FM-FBGs with polymethyl pentane (PMP) coating and without coating with external refractive index 1.3159</i>	82

<b>Fig. 5.13</b>	<b>(a)</b> Reflection spectra of LP <sub>01</sub> & LP <sub>11</sub> mode and coupling between LP <sub>01</sub> -LP <sub>02</sub> mode with a grating length <b>(b)</b> Variation of FWHM with grading length for LP <sub>01</sub> and LP <sub>11</sub> mode	83
<b>Fig. 6.1</b>	<b>(a)</b> Guided mode in guided structure and <b>(b)</b> leaky mode in leaky structure, inset show the oscillating field in leaky layer	88
<b>Fig. 6.2</b>	Computing leaky mode in leaky optical fiber structure	90
<b>Fig. 6.3</b>	Refractive index profile for trench-assisted step index fiber with $r_c = 3.75\mu\text{m}$ , $r_t = 11.25\mu\text{m}$ , $n_1 = 1.4436$ and $n_2 = 1.4436$	93
<b>Fig. 6.4</b>	<b>(a)</b> Modal and <b>(b)</b> propagated field of LP <sub>01</sub> mode in depressed inner cladding fiber	94
<b>Fig. 6.5</b>	Shift in $\delta n_{eff}$ for LP <sub>01</sub> mode in depressed inner cladding fiber at different wavelengths	95
<b>Fig. 6.6</b>	<b>(a)</b> Approximation of outer layer index for LP <sub>01</sub> mode <b>(b)</b> approximation of outer layer index for LP <sub>11</sub> mode and propagation of LP <sub>11</sub> mode through actual depressed inner clad fiber.	97
<b>Fig. 6.7</b>	Refractive index profile of trench-assisted large mode area single mode fiber.	98
<b>Fig. 6.8</b>	Propagation of <b>(a)</b> LP <sub>01</sub> and <b>(b)</b> LP <sub>11</sub> mode in trench assisted large mode area single mode fiber	99
<b>Fig. 6.9</b>	LP <sub>01</sub> and LP <sub>11</sub> modal field intensity with propagation distance.	99
<b>Fig. 7.1</b>	Schematic of Bragg fiber	102
<b>Fig. 7.2</b>	Fundamental mode of Bragg fiber at $\lambda = 1.064\mu\text{m}$ and refractive index profile.	101

<b>Fig. 7.3</b>	<b>(a)</b> <i>Modal and propagated LP<sub>01</sub> mode of Bragg fiber at <math>\lambda = 1.064 \mu\text{m}</math></i>	104
	<b>(b)</b> <i>effective index of fundamental mode of Bragg fiber with wavelength</i>	
<b>Fig. 7.4</b>	<i>Propagation loss/power in the core after 4.5 cm distance of propagation at 1.55 <math>\mu\text{m}</math> wavelength</i>	105
<b>Fig. 7.5</b>	<b>(a)</b> <i>Model field intensity at <math>\lambda = 1.064 \mu\text{m}</math> with and without optimization of layers</i>	106
	<b>(b)</b> <i>effective index of fundamental mode of Bragg fiber with and without optimization of layers of Bragg fibers.</i>	
<b>Fig. 7.6</b>	<i>Propagation loss and fractional power in the core after 4.5 cm distance of propagation at 1.55 <math>\mu\text{m}</math> wavelength with and without optimization of thickness of layers.</i>	107
<b>Fig. 7.7</b>	<b>(a)</b> <i>Input Gaussian beam and output Beam</i>	109
	<b>(b)</b> <i>Propagation of Gaussian beam through Bragg fiber and leakage out of other higher order modes in few micrometers.</i>	
<b>Fig. 7.8</b>	<i>Fractional power in core with input Gaussian beam with wavelength</i>	109
<b>Fig. 7.9</b>	<i>Large core Bragg fiber with liquid core (water) and enlarged part show the high and low refractive index multilayers</i>	110
<b>Fig. 7.10</b>	<i>Refractive index profile of very large liquid core (water) Bragg fiber in transformed and real space</i>	110
<b>Fig. 7.11</b>	<i>Different regions according to rapid and slow variation of refractive index</i>	113
<b>Fig. 7.12</b>	<i>Mapping of refractive index in different regions from real space to transformed space</i>	113
<b>Fig. 7.13</b>	<i>Redistribution of collocation points using variable transformation</i>	114

<b>Fig. 7.14</b>	<i>Transformation and its derivative to model the large core Bragg fiber using variable transformed collocation method.</i>	116
<b>Fig. 7.15</b>	<i>Fundamental mode of Bragg fiber, inset shows the oscillatory field in Layers</i>	117
<b>Fig. 7.16</b>	<i>Transformation with collocation points</i>	117
<b>Fig. 7.17</b>	<i>Redistribution of <math>N=100</math>, collocation points in desired region</i>	118

## LIST OF TABLES

---

Table No.	Description of Table	Page No.
5.1	<i>Various sensitivities for LP<sub>01</sub> and LP<sub>11</sub> modes were obtained experimentally and through our simulation.</i>	79
5.2	<i>Thermal expansion coefficient, Young's modulus of elasticity and cross-sectional area for the fiber core (Germania dopped silica) and Polymethyl pentane (PMP) layer.</i>	81
6.1	<i>Procedure for obtaining effective refractive index of just guiding mode in leaky structures.</i>	89
6.2	<i>Convergence of effective index of mode at <math>\lambda=1.5\mu\text{m}</math> in LP<sub>01</sub> depressed inner cladding fiber.</i>	93
6.3	<i>Successive approximations for the index of the outer layer for the LP<sub>01</sub> mode at different wavelengths.</i>	95
6.4	<i>Comparison of effective index and loss at different wavelengths.</i>	96
6.5	<i>Convergence of the effective index for LP<sub>01</sub> &amp; LP<sub>11</sub> leaky mode in Few-Mode Depressed Inner Cladding Fiber.</i>	97
6.6	<i>Effective refractive index and loss for LP<sub>01</sub> and LP<sub>11</sub> mode in Few-Mode Depressed Inner Cladding Fiber.</i>	98
7.1	<i>Thickness of first three layers with optimization</i>	106
7.2	<i>Effective Index versus number of collocation points using simple collocation method and variable transform collocation method</i>	119